

We are IntechOpen, the world's leading publisher of Open Access books Built by scientists, for scientists

5,800

Open access books available

142,000

International authors and editors

180M

Downloads

Our authors are among the

154

Countries delivered to

TOP 1%

most cited scientists

12.2%

Contributors from top 500 universities



WEB OF SCIENCE™

Selection of our books indexed in the Book Citation Index
in Web of Science™ Core Collection (BKCI)

Interested in publishing with us?
Contact book.department@intechopen.com

Numbers displayed above are based on latest data collected.
For more information visit www.intechopen.com



Chapter

Ramjet Acceleration of Microscopic Black Holes within Stellar Material

Mikhail V. Shubov

Abstract

In this work, we present a case that Microscopic Black Holes (MBH) of mass 10^{16} kg– 3×10^{19} kg experience acceleration as they move within stellar material at low velocities. The accelerating forces are caused by the fact that an MBH moving through stellar material leaves a trail of hot rarefied gas. The rarefied gas behind an MBH exerts a lower gravitational force on the MBH than the dense gas in front of it. The accelerating forces exceed the gravitational drag forces when MBH moves at Mach number $\mathcal{M} < \mathcal{M}_0 < 1$. The equilibrium Mach number \mathcal{M}_0 depends on MBH mass and stellar material characteristics. Our calculations open the possibility of MBH orbiting within stars including the Sun at Mach number \mathcal{M}_0 . At the end of this work, we list some unresolved problems which result from our calculations.

Keywords: primordial black holes, microscopic black holes, ramjet acceleration, accretion, intrastellar orbits

1. Introduction

In the research presented in the works [1–3], it has been suggested that Primordial Black Holes make up a significant fraction of dark matter. Microscopic Black Holes (MBH) can also be formed within stars by coalescence of dark matter composed of weakly interacting massive particles [4, 5]. According to the plot in ([3], p. 14), considerations other than stellar capture constrain the masses of MBH as a dark matter to the range of 10^{16} kg– 5×10^{21} kg.

Up to now, researchers believed that all MBH captured by a star would be slowed down within stellar material until they settle in the stellar center [1, 2]. In the present work, we explore the possibility of MBH accelerating during their passage through stellar matter at low Mach numbers. As MBH passes through matter, it accretes material at a rate we denote \dot{M} . Some of the mass accreted by MBH is turned into energy. This energy escapes the MBH in the form of protons and gamma rays. These rays heat the surrounding material, causing its rarefaction. The rarefied material behind the moving MBH exerts a lower gravitational pull on the MBH than the dense material in front of it. *Moving MBH experiences a net forward force.* This force is called **MBH ramjet force**. The effect is illustrated in **Figure 1**.

The conditions under which MBH accelerates within the stellar material are derived in this work. In order to define these conditions, three efficiencies must be

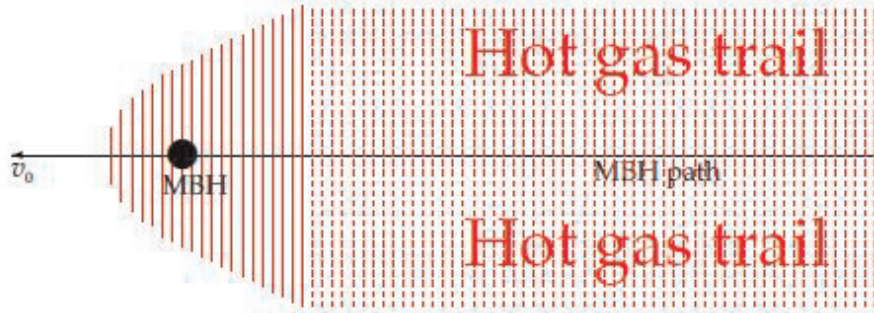


Figure 1.
MBH passage through matter.

defined. These are gas redistribution efficiency, radiative efficiency, and accretion efficiency. **Gas redistribution efficiency**, η_G , is the ratio of the accelerating force caused by gas rarefaction behind the MBH to the theoretical maximum of such force. The exact definition starts at paragraph containing Eq. (9) and ends with a paragraph containing Eq. (11). **Radiative efficiency**, η_Γ , is the ratio of the total power radiated by MBH to the power ($\dot{M}c^2$) of the mass falling into MBH. It is expressed in Eq. (12). **Accretion efficiency**, η_A , is the ratio of the actual and the zero-radiation mass capture rates. It is defined in Eq. (16).

We show that in the case of MBH moving through stellar material at supersonic (supersonic MBH) speed, the condition for MBH acceleration is given in Eq. (29):

$$\mathcal{N} = \frac{\eta_A \eta_\Gamma \eta_{G_2}}{T_6} \gtrsim 4 \cdot 10^{-4} (1 + \mathcal{M}^{-2})^{3/2}, \quad (1)$$

where T_6 is the temperature of the stellar material in millions Kelvin. Even though we do not have precise values for efficiencies η_A , η_Γ , and η_G , we are almost certain that for supersonic MBH, condition Eq. (1) is never met. In the case of MBH moving through stellar material at a subsonic speed (subsonic MBH), the condition for MBH acceleration is given in Eq. (33):

$$\mathcal{N} = \frac{\eta_A \eta_\Gamma \eta_{G_2}}{T_6} \gtrsim 9 \cdot 10^{-7} \mathcal{M}^3 \mathfrak{F}(\mathcal{M}, \eta_A), \quad (2)$$

where \mathcal{M} is the Mach number and $\mathfrak{F}(\mathcal{M}, \eta_A) > 0.11$ is given in Eq (34). Supersonic MBH always experiences deceleration within stellar material. Subsonic MBH experiences acceleration when the Mach number exceeds \mathcal{M}_0 (the equilibrium Mach number) and deceleration when the Mach number is below \mathcal{M}_0 . Eventually the MBH settles into an intrastellar orbit with Mach number \mathcal{M}_0 . The value of \mathcal{M}_0 can be obtained by solving Eq. (2) as an equality.

In Appendix A, a minimal value of η_G for subsonic MBH is estimated. Estimating η_G for supersonic MBH remains an open problem. Calculating the values of η_A and η_Γ also remain open problems. As we discuss later in this work, different theorists obtained different results for η_Γ .

We briefly outline the content of the present chapter. In Section 2, we calculate forces acting on MBH. We also derive conditions for MBH acceleration at subsonic and supersonic speed. In Section 3, we present estimates for η_A and η_Γ . In Section 4, we present an empirical discussion of possible behaviors of MBH within stellar material. In Section 5, the problems remaining after this work are briefly described.

2. Forces acting on an MBH passing through matter

2.1 Total force acting on an MBH

Three forces act on a black hole, which passes through stellar material. The first force denoted by F_t is the tidal or gravitational drag. For a supersonic MBH, F_t is given by ([6], p. 8)

$$F_t = -\frac{1}{v_0} P_t = -\frac{4\pi(MG)^2 \rho}{v_{0_2}} \ln \left(\frac{r_{\max}}{r_{\min}} \right), \quad (3)$$

where P_t is the decelerating power produced by the drag force, ρ is the density of the surrounding medium, r_{\max} is the approximate distance from the MBH to the farthest location where the stellar material is consistent, and r_{\min} is the radius at which matter is initially unperturbed by the MBH radiation. In Eq. (3), M is the mass of the MBH. We take r_{\max} to be about $5 \cdot 10^7$ m for a Sun-like star. We take r_{\min} to be about 0.1 m. Hence,

$$\ln \left(\frac{r_{\max}}{r_{\min}} \right) \approx 20. \quad (4)$$

For an MBH traveling at Mach number $\mathcal{M} \lesssim 0.8$, the gravitational drag can be given by the following formula (see [7], p. 5, [8], p. 69, [9], p. 8)

$$F_t = -\frac{4\pi(MG)^2 \rho}{v_{0_2}} \left[\frac{1}{2} \ln \left(\frac{1 + \mathcal{M}}{1 - \mathcal{M}} \right) - \mathcal{M} \right]. \quad (5)$$

Since $\mathcal{M} < 1$, Eq. (5) can be rewritten in the form of a converging series

$$F_t = -\frac{4\pi(MG)^2 \rho}{v_{0_2}} \sum_{n=1}^{\infty} \frac{\mathcal{M}^{2n+1}}{2n+1}. \quad (6)$$

The second force is drag caused by mass acquisition. As the MBH passes through stellar material, it consumes mass that was formerly at rest. MBH momentum does not change as a result of mass acquisition. Change of MBH speed can be calculated from conservation of momentum:

$$\frac{\partial p}{\partial t} = \frac{\partial}{\partial t} (Mv_0) = \dot{M}v_0 + M\dot{v}_0 = 0 \quad \Rightarrow \quad \dot{v}_0 = -v_0 \frac{\dot{M}}{M}. \quad (7)$$

Using MBH speed change, we calculate the effective force as

$$F_m = M \frac{\partial v_0}{\partial t} = -\dot{M}v_0. \quad (8)$$

The third force is accelerative. It is caused by matter rarefaction behind the moving MBH. This force is denoted by F_r . In order to estimate F_r , we need two radii, r_1 and r_2 . The radius r_1 is defined in terms of F_r . A sphere of gas directly behind the MBH having radius r_1 , and density $\rho/2$ would cause the MBH to experience accelerative force F_r . The sphere of rarefied gas behind an MBH acts as a sphere with a negative

density of $\rho/2 - \rho = -\rho/2$. The accelerating “ramjet” force F_r acting on the MBH expressed in terms of r_1 is:

$$F_r = -\frac{MM_s G}{r_{1_2}} = MG \frac{\frac{1}{2} \frac{4}{3} \pi r_{1_3} \rho}{r_{1_2}} = \frac{2}{3} \pi MG \rho r_1, \quad (9)$$

where M_s is the effective negative mass of the sphere of rarefied gas.

The radius r_2 is defined in terms of the power P radiated by MBH passing through the stellar material. Imagine that power P is used to uniformly heat a cylinder of stellar material along the path of MBH. The MBH moves at speed v_0 . The radius r_2 is defined as the radius of the aforementioned cylinder for which the temperature of gas contained in it would double. Then the relation between P and r_2 is:

$$P = (\text{Mass heated per unit of time}) \cdot T \cdot C_v = v_0 (\pi r_{2_2} \rho) T \cdot C_v = \pi v_0 \rho T C_v r_{2_2}, \quad (10)$$

where C_v is the heat capacity of gas of stellar material at constant volume.

The **gas redistribution efficiency** is defined as

$$\eta_G = \frac{r_1}{r_2}. \quad (11)$$

As we show later in this section, the ramjet force F_r acting on MBH is proportional to η_G . The minimal value for η_G for subsonic MBH is estimated in Appendix A.

The radiative power of the MBH passing through stellar material is

$$P = \eta_r c^2 \dot{M}, \quad (12)$$

where η_r is the **radiative efficiency** of MBH and \dot{M} is the mass accretion rate. For a supersonic MBH, the Bondi-Hoyle-Lyttleton accretion rate is ([10], p. 203)

$$\dot{M}_{BH} = 4\pi r_b \rho \sqrt{v_{0_2} + v_{s_2}}, \quad (13)$$

where r_b is the Bondi radius, and v_s is the sound speed in the stellar material. The Bondi radius is ([10], p. 203)

$$r_b = \frac{MG}{v_{s_2} + v_0}. \quad (14)$$

Substituting Eq. (14) into Eq. (13), we obtain

$$\dot{M}_{BH} = 4\pi r_b^2 \rho v_0 = \frac{4\pi (MG)^2 \rho}{(v_0^2 + v_s^2)^{3/2}}. \quad (15)$$

The actual mass capture rate is considerably smaller. The radiative heating of the gas surrounding MBH increases its temperature. This increases the gas sound speed and decreases gas density. Thus, the actual mass capture rate is

$$\dot{M} \approx \frac{4\pi (MG)^2 \rho_r}{(v_0^2 + v_{sr}^2)^{3/2}}, \quad (16)$$

where v_{sr} is the sound speed at the accretion radius and ρ_r is the density at the accretion radius. Recall the **accretion efficiency** η_A is the quotient of actual and zero-radiation mass capture rates:

$$\eta_A = \frac{\dot{M}}{\dot{M}_{BH}} \approx \left(\frac{v_{0_2} + v_{s_2}}{v_{0_2} + v_{sr_2}} \right)^{3/2} \frac{\rho_r}{\rho}. \quad (17)$$

Equating the power from Eqs. (10) and (12), we obtain

$$\pi v_0 \rho T C_v r_2 = \eta_A c^2 \dot{M}. \quad (18)$$

Substituting Eqs. (15) and (16) into Eq. (18), we obtain

$$\pi v_0 \rho T C_v r_2 = \eta_A c^2 \eta_A \frac{4\pi(MG)^2 \rho}{(v_{0_2} + v_{s_2})^{3/2}}. \quad (19)$$

Thus,

$$r_2 = 2\sqrt{\eta_A} \sqrt{\frac{\eta_A c^2}{T C_v} \frac{MG}{(v_{0_2} + v_{s_2})^{3/4} \sqrt{v_0}}} = 2\sqrt{\frac{\eta_A \eta_A c^2 MG}{T C_v v_{0_2}} \left(1 + \frac{v_{s_2}}{v_{0_2}}\right)^{-3/4}}. \quad (20)$$

Substituting Eq. (20) into Eq. (11), we obtain an expression for r_1 :

$$r_1 = 2\eta_G \sqrt{\frac{\eta_A \eta_A c^2 MG}{T C_v v_{0_2}} \left(1 + \frac{v_{s_2}}{v_{0_2}}\right)^{-3/4}}. \quad (21)$$

At this point, we calculate the second and the third forces acting on the MBH. The first one is given in Eq. (3) for a supersonic MBH and in Eq. (5) for a subsonic MBH. Substituting Eq. (21) into Eq. (9), we obtain

$$F_r = \frac{2}{3} \pi M G \rho r_1 = \left[\frac{4}{3} \eta_G \sqrt{\frac{\eta_A \eta_A c^2}{T C_v} \left(1 + \frac{v_{s_2}}{v_{0_2}}\right)^{-3/4}} \right] \frac{\pi(MG)^2 \rho}{v_{0_2}}. \quad (22)$$

Substituting Eqs. (15) and (16) into Eq. (8), we obtain

$$\begin{aligned} F_m &= -\dot{M} v_0 = -\eta_A \dot{M}_{BH} v_0 = -\eta_A \frac{4\pi(MG)^2 \rho}{(v_{0_2} + v_{s_2})^{3/2}} v_0 \\ &= -4\eta_A \left(1 + \frac{v_{s_2}}{v_{0_2}}\right)^{-3/2} \frac{\pi(MG)^2 \rho}{v_{0_2}}. \end{aligned} \quad (23)$$

2.2 Conditions for supersonic MBH acceleration

The total force acting on a supersonic MBH is obtained by summing Eqs. (3), (22) and (23):

$$\begin{aligned}
 F &= F_t + F_m + F_r \\
 &= \frac{\pi(MG)^2 \rho}{v_{0_2}} \left[-4 \ln \left(\frac{r_{\max}}{r_{\min}} \right) - 4\eta_A \left(1 + \frac{v_{s_2}}{v_{0_2}} \right)^{-3/2} + 2\eta_G \sqrt{\frac{\eta_A \eta_\Gamma c^2}{TC_v}} \left(1 + \frac{v_{s_2}}{v_{0_2}} \right)^{-3/4} \right].
 \end{aligned} \tag{24}$$

The above equation shows that MBH accelerates if and only if $F > 0$, i.e.

$$\eta_G \sqrt{\frac{\eta_A \eta_\Gamma c^2}{TC_v}} \left(1 + \frac{v_{s_2}}{v_{0_2}} \right)^{-3/4} > 2 \ln \left(\frac{r_{\max}}{r_{\min}} \right) + 2\eta_A \left(1 + \frac{v_{s_2}}{v_{0_2}} \right)^{-3/2}. \tag{25}$$

In this subsection we estimate conditions under which the MBH passing through matter accelerates, i.e., Eq. (25) holds. This condition can be rewritten as

$$\eta_A \eta_\Gamma \eta_{G_2} > \frac{4TC_v}{c^2} \left[\ln \left(\frac{r_{\max}}{r_{\min}} \right) + \eta_A \left(1 + \frac{v_{s_2}}{v_{0_2}} \right)^{-3/2} \right]^2 \left(1 + \frac{v_{s_2}}{v_{0_2}} \right)^{3/2} \tag{26}$$

Recalling Eq. (4), and the fact that $\eta_A < 1$, we rewrite the estimate to Eq. (26) as

$$\eta_A \eta_\Gamma \eta_{G_2} \gtrsim 1.7 \cdot 10^3 \cdot \frac{TC_v}{c^2} \left(1 + \frac{v_{s_2}}{v_{0_2}} \right)^{3/2} = 1.7 \cdot 10^3 \cdot \frac{TC_v}{c^2} (1 + \mathcal{M}^{-2})^{3/2}. \tag{27}$$

The heat capacity at the constant volume of a monatomic gas is

$$C_v = \frac{3R}{2m_a}, \tag{28}$$

where m_a is the average molar mass of the gas, and R is the gas constant ($R = 8.314 \frac{J}{\text{mol}^\circ K}$). Typical stellar material consists of monatomic gas with an average particle mass of 0.62 amu ([11], p. 378). Hence, the heat capacity at constant volume for stellar material is $C_v = 2.01 \cdot 10^4 \frac{J}{\text{kg}^\circ K}$. Thus, Eq. (27) can be rewritten as

$$\mathcal{N} = \frac{\eta_A \eta_\Gamma \eta_{G_2}}{T_6} \gtrsim 4 \cdot 10^{-4} (1 + \mathcal{M}^{-2})^{3/2}. \tag{29}$$

As we show in Subsection 3.2, η_A is very small if the temperature of the gas at Bondi radius is high. As we discuss in Subsection 3.3, different calculations of η_Γ in previous works yield different results, yet all of them are below 0.1. For supersonic MBH, η_G should rapidly decrease with increasing Mach number. We have only qualitative arguments regarding the values of η_G . Stellar matter behind the MBH, which is displaced by a heat wave, remains within the Mach cone. Its gravitational pull can not be much lower than the pull of the unaffected matter in front of MBH. As the MBH Mach number increases, the cone becomes narrower. The difference of gravitational pull between matter in front of MBH and behind MBH decreases. Hence, η_G decreases as well. Calculation of η_G is beyond the scope of this work. The solar gas temperature exceeds $T_6 = 4$ for radius under 0.5 Solar radii [11].

Based on the above data, we can be almost certain that relation Eq. (29) does not hold for Mach numbers $\mathcal{M} > 1$, thus a supersonic MBH can not accelerate. **Very**

extensive analysis is needed in order to rigorously prove this assertion. Such analysis is beyond the scope of this work. It may be beyond the scope of any previous work on black hole accretion.

2.3 Conditions for subsonic MBH acceleration

The tidal decelerating force acting on an MBH traveling through stellar material at Mach number $\mathcal{M} \lesssim 0.8$ is given by Eq. (6). The total force acting on MBH is obtained by summing Eqs. (6), (22), and (23):

$$\begin{aligned}
 F &= F_t + F_m + F_r \\
 &= \frac{\pi(MG)^2 \rho}{v_{0_2}} \left[-4 \sum_{n=1}^{\infty} \frac{\mathcal{M}^{2n+1}}{2n+1} - 4\eta_A \left(1 + \frac{v_{s_2}}{v_{0_2}}\right)^{-3/2} + 2\eta_G \sqrt{\frac{\eta_A \eta_{\Gamma} c^2}{TC_v}} \left(1 + \frac{v_{s_2}}{v_{0_2}}\right)^{-3/4} \right] \\
 &= \frac{\pi(MG)^2 \rho}{v_{0_2}} \left[-4 \sum_{n=1}^{\infty} \frac{\mathcal{M}^{2n+1}}{2n+1} - 4\eta_A \left(1 + \frac{1}{\mathcal{M}^2}\right)^{-3/2} + 2\eta_G \sqrt{\frac{\eta_A \eta_{\Gamma} c^2}{TC_v}} \left(1 + \frac{1}{\mathcal{M}^2}\right)^{-3/4} \right].
 \end{aligned} \tag{30}$$

The above equation shows that MBH will accelerate if and only if $F > 0$ or

$$\eta_G \sqrt{\frac{\eta_A \eta_{\Gamma} c^2}{TC_v}} (1 + \mathcal{M}^{-2})^{-3/4} > 2 \sum_{n=1}^{\infty} \frac{\mathcal{M}^{2n+1}}{2n+1} + 2\eta_A (1 + \mathcal{M}^{-2})^{-3/2}. \tag{31}$$

Rewrite Eq. (31) as:

$$\begin{aligned}
 \eta_A \eta_{\Gamma} \eta_{G_2} &> \frac{4TC_v}{c^2} (1 + \mathcal{M}^{-2})^{3/2} \left[\sum_{n=1}^{\infty} \frac{\mathcal{M}^{2n+1}}{2n+1} + \eta_A (1 + \mathcal{M}^{-2})^{-3/2} \right]^2 \\
 &= \frac{4TC_v}{c^2} \mathcal{M}^3 \left\{ (1 + \mathcal{M}^2)^{3/2} \left[\sum_{n=0}^{\infty} \frac{\mathcal{M}^{2n}}{2n+3} + \eta_A (1 + \mathcal{M}^2)^{-3/2} \right]^2 \right\}.
 \end{aligned} \tag{32}$$

Given that $C_v = 2.01 \cdot 10^4 \frac{J}{kg^{\circ}K}$, we rewrite Eq. (32) as

$$\frac{\eta_A \eta_{\Gamma} \eta_{G_2}}{T_6} \gtrsim 9 \cdot 10^{-7} \mathcal{M}^3 \mathfrak{F}(\mathcal{M}, \eta_A), \tag{33}$$

where

$$\mathfrak{F}(\mathcal{M}, \eta_A) = (1 + \mathcal{M}^2)^{3/2} \left[\sum_{n=0}^{\infty} \frac{\mathcal{M}^{2n}}{2n+3} + \eta_A (1 + \mathcal{M}^2)^{-3/2} \right]^2. \tag{34}$$

Notice that $\mathfrak{F}(\mathcal{M}, \eta_A) > .11$.

The Mach number for which an MBH settles into a stable intrastellar orbit is such that the net force acting on the MBH is 0. It can be estimated by solving an equation derived from Eq. (33):

$$\mathcal{N} = \frac{\eta_A \eta_\Gamma \eta_{G_2}}{T_6} = 9 \cdot 10^{-7} \mathcal{M}^3 \mathfrak{F}(\mathcal{M}, \eta_A). \quad (35)$$

All three efficiencies in Eq. (35) are nonzero. Thus, Eq. (35) does have a solution \mathcal{M}_0 . An MBH traveling in stellar material accelerates when its Mach number is below \mathcal{M}_0 and decelerates when its Mach number is above \mathcal{M}_0 . Thus, an MBH traveling within a star is bound to settle into a stable intrastellar orbit. In order to calculate \mathcal{M}_0 from Eq. (35), one must know gas redistribution, accretion and radiative efficiencies. In the next section, we present preliminary estimates for the three aforementioned efficiencies.

3. Estimation of gas redistribution, accretion and radiative efficiencies

3.1 The value of η_G

In Appendix A.1, we prove that

$$\eta_G = \frac{r_1}{r_2} \geq .44 \sqrt{\frac{K-1}{K}} \quad (36)$$

for MBH traveling at subsonic speeds with $\mathcal{M} < 0.8$. K is the ratio of average temperature in the hot gas trail and ambient temperature of stellar material. A possible route for estimating K is outlined in Appendix A.2.

3.2 The value of η_A

From Eq. (17), we estimate η_A as

$$\eta_A \approx \left(\frac{v_{0_2} + v_{s_2}}{v_{0_2} + v_{sr_2}} \right)^{3/2} \frac{\rho_r}{\rho}, \quad (37)$$

where v_{sr} is the sound speed at the accretion radius and ρ_r is the density at the accretion radius. Given that gas density is proportional to its pressure divided by temperature, we obtain

$$\begin{aligned} \eta_A &\approx \left(\frac{v_{0_2} + v_{s_2}}{v_{0_2} + v_{sr_2}} \right)^{3/2} \frac{\rho_r}{\rho} = \left(\frac{v_{0_2} + v_{s_2}}{v_{0_2} + v_{sr_2}} \right)^{3/2} \frac{\mathbf{P}_r T}{\mathbf{P} T_r} = \left(\frac{(v_0/v_s)^2 + 1}{(v_0/v_s)^2 + (v_{sr}/v_s)^2} \right)^{3/2} \frac{\mathbf{P}_r T}{\mathbf{P} T_r} \\ &= \left(\frac{\mathcal{M}^2 + 1}{\mathcal{M}^2 + (v_{sr}/v_s)^2} \right)^{3/2} \frac{\mathbf{P}_r T}{\mathbf{P} T_r}. \end{aligned} \quad (38)$$

In Eq. (38), T is the ambient temperature of stellar material, and T_r is the temperature of stellar material at Bondi radius. The ambient pressure is \mathbf{P} , and pressure at Bondi radius is \mathbf{P}_r . Notation P can not be used for pressure, as it is already used for power. For a gaseous medium, the sound velocity is proportional to the square root of temperature. Thus,

$$\left(\frac{v_{sr}}{v_s}\right)^2 = \frac{T_r}{T}. \quad (39)$$

Substituting Eq. (39) into Eq. (38), we obtain the approximation

$$\eta_A \approx \left(\frac{\mathcal{M}^2 + 1}{\mathcal{M}^2 + T_r/T}\right)^{3/2} \frac{\mathbf{P}_r T}{\mathbf{P} T_r}. \quad (40)$$

The pressure within the immediate vicinity of MBH should be approximated by the sum of gas pressure and dynamic pressure:

$$\mathbf{P}_r = \mathbf{P} + \frac{\rho v_{0_2}}{2} = \mathbf{P} + \rho v_{s_2} \frac{\mathcal{M}^2}{2}. \quad (41)$$

Notice that the gas density at the Bondi radius must be equal to or lower than the density of unperturbed gas. Hence, the approximation in Eq. (41) above works only when

$$\frac{\mathbf{P}_r T}{\mathbf{P} T_r} < 1, \quad (42)$$

The relation between pressure and sound velocity in a monatomic ideal gas is ([12], p. 683):

$$\mathbf{P} = \frac{\rho v_{s_2}}{\gamma} = \frac{3}{5} \rho v_{s_2}. \quad (43)$$

Substituting Eq. (43) into Eq. (41), we obtain the pressure ratio

$$\frac{\mathbf{P}_r}{\mathbf{P}} = \frac{\frac{3}{5} \rho v_{s_2} + \rho v_{s_2} \frac{\mathcal{M}^2}{2}}{\frac{3}{5} \rho v_{s_2}} = 1 + \frac{5}{6} \mathcal{M}^2. \quad (44)$$

Substituting Eqs. (44) and (42) into Eq. (40), we obtain

$$\eta_A \approx \left(\frac{\mathcal{M}^2 + 1}{\mathcal{M}^2 + T_r/T}\right)^{3/2} \min \left\{ 1, \left(1 + \frac{5}{6} \mathcal{M}^2\right) \frac{T}{T_r} \right\}. \quad (45)$$

As we see, η_A is a rapidly increasing function of the Mach number and a rapidly decreasing function of T_r/T . For subsonic MBH and for all cases where $T_r/T \gg \mathcal{M}^2$, Eq. (45) can be approximated as

$$\eta_A \approx \left(1 + \frac{5}{6} \mathcal{M}^2\right) (\mathcal{M}^2 + 1)^{3/2} \left(\frac{T}{T_r}\right)^{5/2}. \quad (46)$$

Calculation of T_r remains an unsolved problem.

3.3 The value of η_r

Some energy is radiated from a spherically accreting MBH in the form of photons. The power radiated as photons is given as $\eta_r \dot{M} c^2$. Some energy is radiated from a

spherically accreting MBH in the form of protons and neutrons. The power radiated as baryons is given as $\eta_p \dot{M} c^2$, since protons are more numerous than neutrons. The overall radiative efficiency of an MBH is

$$\eta_{\Gamma} = \eta_{\gamma} + \eta_p. \quad (47)$$

3.3.1 Gamma radiation from spherically accreting MBH

Accretion rate per unit MBH mass is one of the main factors determining η_{γ} . This rate should be expressed as a multiple of the Eddington accretion rate ([13], p. 51):

$$\mathfrak{A} = \frac{(1.43 \cdot 10^{16} \text{ s}) \dot{M}}{M} = \frac{\dot{M}}{\left(70 \frac{\text{kg}}{\text{s}}\right) M_{18}}, \quad (48)$$

where M_{18} is the mass of MBH in units of 10^{18} kg.

Below we will summarize some previous works calculating η_{γ} for spherical accretion. Spherical accretion on black holes have been studied theoretically, with different theories producing different values of radiative efficiency (η_{γ}) ([13], p. 25–55). Radiative efficiencies ranging from 10^{-10} to over .1 have been obtained for different parameters. The magnetic field greatly increases η_{γ} ([13], p. 34–35). For $10^{-4} \leq \mathfrak{A} \leq 1$, radiative efficiency can be as high as 0.1 if the flow is turbulent ([13], p. 35).

Detailed calculations of spherical accretion are presented in Ref. [14]. For a black hole of $2 \cdot 10^{38}$ kg, radiative efficiency starts growing almost from zero at $\mathfrak{A} = .02$ and reaches $\eta_{\gamma} = .19$ for $\mathfrak{A} = 1.2$. For a black hole of $2 \cdot 10^{31}$ kg, radiative efficiency starts growing almost from zero at $\mathfrak{A} = .5$ and reaches $\eta_{\gamma} = .15$ for $\mathfrak{A} = .12$. MBH was not considered.

A model which considers separate ion and electron temperatures within accreting gas is given in Ref. [15]. Black hole masses between 2×10^{31} kg and 2×10^{38} kg are considered. Accretion rates between $\mathfrak{A} = 7 \cdot 10^{-3}$ and $\mathfrak{A} = 2$ are considered. In all cases, the efficiency stays within $\eta_{\gamma} \in [4.8 \cdot 10^{-3}, 7 \cdot 10^{-3}]$. Notice, that all of the aforementioned studies considered black holes many orders of magnitude heavier than 10^{18} kg. To obtain better results for MBH, more detailed studies for black holes within 10^{16} kg– 3×10^{19} kg are needed.

For black holes with accretion rates $\mathfrak{A} \in (1, 300)$, the values of η_{γ} range from 10^{-6} to 10^{-2} ([16], p.10). The state-of-the-art results have a lot of uncertainty.

3.3.2 Proton and neutron radiation from spherically accreting MBH

Gas accreting toward MBH experiences great compression, which causes adiabatic heating. Hot gas reaches temperatures of tens to hundreds of billion degrees Kelvin. As a result, some protons and neutrons which have excess energy escape the gravitational well around MBH. A very rudimentary estimation of η_p is performed below. In order to calculate η_p precisely, we would need to perform an extensive Monte Carlo simulation. This simulation would have to take into account proton motion and collisions.

During accretion, the electron gas is much colder than the proton gas. Average temperature of proton is approximated by ([14], p. 17, [15], p. 323):

$$T(yr_s) = \frac{T_s}{y}, \quad (49)$$

where r_s is the Schwarzschild radius and $T_s \approx 10^{12} K$. When the distance from MBH is corresponding to $y \in (25, 50)$ Schwarzschild radii and the gas temperature is 20–40 billion Kelvin, the nuclei split into protons and neutrons.

At this point, we calculate the depth of the potential well in which nucleons appear at a distance (yr_s) from the MBH center. We take the non-relativistic approximation valid for $y \geq 2$.

$$E_p(yr_s) = -\frac{m_p MG}{yr_s} = -\frac{m_p MG}{y \frac{2MG}{c^2}} = -\frac{m_p c^2}{2y}, \quad (50)$$

where m_p is the proton mass. Below, we express Eq. (50) in terms of Boltzmann constant $k = 1.381 \times 10^{-23}$ J/K:

$$E_p(yr_s) = -\frac{m_p c^2}{2y} = -\frac{k}{y} \cdot \frac{m_p c^2}{2k} = -5.44 \cdot 10^{12} K \frac{k}{y} \approx -\frac{5.44 k T_s}{y}. \quad (51)$$

Like particles of any gas, protons and neutrons within accreting gas should have Maxwell energy distribution:

$$f(E) = \frac{2}{\sqrt{\pi} kT} \sqrt{\frac{E}{kT}} \exp\left(-\frac{E}{kT}\right), \quad (52)$$

At any distance (yr_s) from the MBH center, some nucleons have sufficient kinetic energy to escape from the gravitational potential well of MBH. The energy depth of that well is given by Eq. (51). The fraction of nucleons capable of escaping is

$$\mathcal{F}_e = \int_{5.44}^{\infty} f(E) dE = 0.012. \quad (53)$$

Nucleons escaping from a distance (yr_s) from the MBH center carry excess kinetic energy. That energy is

$$\mathcal{F}_e = \frac{kT_s}{y} \int_{5.44}^{\infty} (E - 5.44) f(E) dE = 0.009 \frac{kT_s}{y}. \quad (54)$$

The energy given in Eq. (54) above is the quotient of the excess energy of ejected nucleons to the total number of nucleons, including the ones not ejected.

Define η_p^* as the quotient of the kinetic energy of nucleons ejected from accreting material to the rest energy of all nucleons. Many ejected nucleons lose energy in collisions, and some return to MBH. Thus, the final energy radiated from MBH as nucleon radiation is $\eta_p < \eta_p^*$. We estimate η_p^* as

$$\frac{d\eta_p^*}{d(\ln y)} = \frac{\mathcal{F}_e(y)}{m_p c^2} = \frac{0.009 kT_s}{m_p c^2} \frac{1}{y} \approx \frac{8 \cdot 10^{-4}}{y}. \quad (55)$$

Integrating Eq. (55) for $y > 2$, we obtain

$$\eta_p^* \approx \int_{y=2}^{\infty} \frac{8 \cdot 10^{-4}}{y} dy = 4 \cdot 10^{-4}. \quad (56)$$

The value of η_p depends on the fraction of the nucleons which are slowed down by accreting gas and returning to MBH. An extensive study and simulation may yield the value of η_p higher than the value of η_p^* estimated in Eq. (56). At this point, precise efficiencies are unknown.

4. Possible modes of interaction of MBH with a star

In this section, we discuss the behavior of a Primordial Black Hole (PBH) which is captured into an orbit that intersects a star. Every PBH discussed here is an MBH, since it is microscopic. Not every MBH is a PBH, since some MBH are not primordial.

PBH ejection from a star-intersecting orbit is the first mode of PBH-star interaction. Any MBH or PBH on a star-intersecting orbit moves within stellar material with supersonic speed. Thus, it experiences deceleration within stellar material. Such MBH or PBH can be ejected from its orbit only by gravitational interaction with the star's planets. In our opinion, such ejections are not rare. Reasoning follows.

Kinetic energy loss of an MBH on a single intrastellar passage is (see Appendix B):

$$\Delta E_{\text{pass}} = (2.0 \cdot 10^{19} \text{ J}) M_{182}. \quad (57)$$

The energy needed to drop the apogee of an elliptic MBH orbit around a sun-like star to 1 Astronomical Unit is

$$\Delta E_{\text{orbit}} = \frac{GM_{\text{Sun}}M_{\text{MBH}}}{1 \text{ AU}} = (8.9 \cdot 10^{26} \text{ J}) M_{18}. \quad (58)$$

Dividing Eq. (58) by Eq. (57), we obtain the number of times an MBH has to pass through a star in order for its orbit to descend to 1 AU:

$$N = \frac{\Delta E_{\text{orbit}}}{\Delta E_{\text{pass}}} \approx 4.5 \cdot 10^7 (M_{18})^{-1}. \quad (59)$$

During this number of passes, the gravity of satellites of a star may throw an MBH off the orbit.

Settling of MBH into an intrastellar orbit is the second mode of MBH-star interaction. One possibility of MBH entering an intrastellar orbit is an MBH is a capture by a star. Another possibility is MBH production at the star center by coalescence of dark matter [4, 5]. Such MBH would be accelerated until it settles in an intrastellar orbit.

Consumption of a host star by an MBH is the third mode of MBH-star interaction. The evolution of an intrastellar MBH depends on its growth rate. An intrastellar MBH moves at low subsonic speed, hence its mass growth rate can be approximated by Eq. (15) which holds for a stationary MBH:

$$\dot{M} = \frac{4\pi(MG)^2 \rho_r}{v_{sr_3}}, \quad (60)$$

where ρ_r is the density at Bondi radius and v_{sr} is the sound speed and Bondi radius. Sound velocity within the gas is proportional to $T^{0.5}$. Gas density is proportional to T^{-1} . Hence,

$$\dot{M} = \frac{4\pi(MG)^2\rho}{v_{s3}} \left(\frac{T}{T_r}\right)^{2.5}, \quad (61)$$

where ρ , v_s , and T are the density, sound speed, and temperature of stellar material, while T_r is the temperature at Bondi radius. In the Solar center, the density is $1.5 \times 10^5 \frac{\text{kg}}{\text{m}^3}$ and the sound speed is $5.1 \times 10^5 \frac{\text{m}}{\text{s}}$ ([11], p. 378). Substituting the above into Eq. (61), we obtain the accretion rate

$$\dot{M} = 6.3 \times 10^4 \frac{\text{kg}}{\text{s}} \left(\frac{T}{T_r}\right)^{2.5} M_{18}^2 = \frac{2 \times 10^{18} \text{ kg}}{\text{Million years}} \left(\frac{T}{T_r}\right)^{2.5} M_{18}^2. \quad (62)$$

Dividing both sides of the above equation by mass, we obtain

$$\frac{d}{dt}(\ln M_{18}) = \frac{\dot{M}_{18}}{M_{18}} = \frac{\dot{M}}{M} = \frac{2M_{18}}{\text{Million years}} \left(\frac{T}{T_r}\right)^{2.5}. \quad (63)$$

In Eq. (63) above, T and T_r are gas temperatures of ambient matter and at Bondi radius respectively. A low mass MBH is unlikely to experience significant growth over the lifetime of the host star. Determining exact MBH and host star characteristics for which the host star is consumed remains an open problem.

As we see from Eq. (63), the initial growth of an MBH within a star is slow. As the MBH gains mass with $M_{18} > 100$, all emitted radiation is absorbed by the accreting gas and $T \approx T_r$. Then the star is consumed by MBH over several millennia.

The growth of intrastellar black holes has been considered by previous researchers [18]. As a black hole consumes a star, it obtains the star's angular momentum and becomes a rapidly rotating black hole. As a rotating black hole absorbs matter, it radiates two jets along its axis [19]. The final stages of stellar consumption by MBH may be responsible for long γ -ray pulses [20].

5. Conclusion and remaining problems

In this work, we have demonstrated that MBH passing through stellar material experiences acceleration rather than deceleration as long as

$$\mathcal{N} = \frac{\eta_A \eta_\Gamma \eta_{G_2}}{T_6} \gtrsim \begin{cases} 4 \cdot 10^{-4} (1 + \mathcal{M}^{-2})^{3/2} & \text{for supersonic MBH} \\ 9 \cdot 10^{-7} \mathcal{M}^3 \mathfrak{F}(\mathcal{M}, \eta_A) & \text{for subsonic MBH} \end{cases}, \quad (64)$$

where $\mathfrak{F}(\mathcal{M}, \eta_A)$ is given in Eq. (34). T_6 is the temperature of the stellar material in millions Kelvin. The **gas redistribution efficiency** η_G , **radiative efficiency** η_Γ , and **accretion efficiency** η_A are defined in Introduction and Section 2.

MBH in stellar material experiences deceleration at supersonic speed. Subsonic MBH either accelerates or decelerates until it reaches equilibrium Mach number calculated from (??) and settles into a stable intrastellar orbit.

If the Universe contains MBH, many or most of them may exist in intrastellar orbits within stars. Some MBH may be orbiting within the Sun. Some of these MBH may be PBH captured by stars. We do not know how frequent is stellar capture of PBH. The calculation of this frequency is one of the many open problems generated by this work. Different PBH masses as well as star and planetary system characteristics will have to be considered in this calculation.

Other MBH may be generated within stellar centers. According to some theories, most Dark Matter consists of Weakly Interacting Massive Particles (WIMPs). Within stellar centers, WIMPs may coalesce into MBH [4, 5]. These MBH would experience acceleration until they settle into intrastellar orbits.

Several detectable effects may be produced by MBH on intrastellar orbits. Some Type 1a supernovas may be triggered by these MBHs [4]. Some MBHs may be on an intrastellar orbit within Sun. These MBH produce very low-frequency sonic waves. These waves are detectable by **helioseismology**—study of vibrations of Solar photosphere.

Only very low frequency sound can travel long distances in any gas. Sound with a frequency of a few millihertz or lower can travel from the Solar center to the Solar surface [22]. From the data presented in Ref. ([11], p. 378) we calculate that the orbital period of an MBH on an intasolar orbit is at least 800 s. This shows that acoustic waves produced by MBH rich Solar surface. Hence, these waves can be detected.

As mentioned in Subsection 3.3, **radiative efficiencies** η_{Γ} of accreting MBH can not be determined at this point. Most advanced theories give results, which vary by several orders of magnitude. Values ranging from 10^{-10} to 0.1 have been obtained so far. We do not know which theory is correct. If one or more MBH orbiting within the Sun is detected, then true values of radiative efficiencies will be obtained from observation.

In Appendix A, we estimate a minimum value of η_G for subsonic MBH. The exact calculation of η_G is a remaining problem. It would involve extensive theoretical work and simulations using gas dynamics and radiation-matter interaction.

Accretion efficiency η_A for both subsonic and supersonic MBH is given by Eq. (45) in terms of T_r —the temperature at the Bondi radius. The calculation of T_r is a remaining problem. Exact calculation of T_r , and η_A would involve extensive theoretical work and simulations using gas dynamics, radiation energy transport, and magnetohydrodynamics.

This work is purely theoretical. Nevertheless, helioseismological observations may eventually provide evidence of an MBH orbiting in an intrasolar orbit. This observation may open possibilities to obtain additional knowledge in many branches of physics. Knowledge in any branch of physics may lead to unforeseeable technological advances in the future.

A. Estimation of bounds on η_G

A.1 Minimum value of η_G for subsonic MBH

We assume strictly subsonic regime with $\mathcal{M} \leq 0.8$. In a diagram below, we illustrate the MBH passing through stellar material.

The heated stellar material produced by subsonic MBH consists of two regions. The first region is the parabolic head region of hot gas surrounding the MBH. The second region is the hot gas trail, denoted by \mathcal{R}_{hg} .

An important issue is the location of stellar material mass displaced by the heat wave. If MBH has subsonic speed, then sonic density waves carry away all of the displaced mass. Sonic waves are shaped as expanding spherical shells. Each shell is centered at the point of wave origin. A subsonic MBH can not outrun shells expanding at the speed of sound. Hence, all of the expanding shells contain advancing MBH inside them. As a result, these shells containing displaced matter exert no net gravitational force on MBH.

Accelerative force F_r exerted on MBH comes from the difference in density of ambient stellar material and hot rarefied gas within the tail region \mathcal{R}_{hg} as well as the head region as shown on **Figure 2**. We simplify calculation by ignoring the head region, which does provide a small propulsive force.

The gravitational force exerted by \mathcal{R}_{hg} is calculated below. The region \mathcal{R}_{hg} can be approximated by a cylinder with radius r_h . This cylinder starts at the distance at most r_h from the MBH. By taking the distance to be r_h , we are estimating the minimal value of the force. The region \mathcal{R}_{hg} is represented in cylindrical coordinates with MBH at the origin. The direction in which the MBH is traveling is $-\hat{z}$. In cylindrical coordinates, \mathcal{R}_{hg} is given by

$$\begin{cases} z \in (r_h, \infty) \\ r \in [0, r_h] \end{cases} \quad (\text{A.1})$$

Stellar gas temperature in \mathcal{R}_{hg} is approximated by a uniform temperature KT , where $K > 1$ is a constant and T is the ambient temperature. Gas pressure within \mathcal{R}_{hg} is almost the same as ambient gas pressure. From temperature and pressure in \mathcal{R}_{hg} , it follows that the gas density in that region is ρ/K , where ρ is the ambient density. From the standpoint of gravitational interaction, **effective negative density** ρ_- of the material in \mathcal{R}_{hg} can be defined as the difference between gas density in \mathcal{R}_{hg} and ambient gas density. Effective negative density is

$$\rho_- = \frac{\rho}{K} - \rho = -\rho \frac{K - 1}{K}. \quad (\text{A.2})$$

The rarefied gas region \mathcal{R}_{hg} exerts the following force on MBH:

$$\mathbf{F} = \iiint_{\mathcal{R}_{hg}} (\rho_-) \mathbf{g}(\mathbf{r}) dV = -\rho \frac{K - 1}{K} \iiint_{\mathcal{R}_{hg}} \mathbf{g}(\mathbf{r}) dV. \quad (\text{A.3})$$

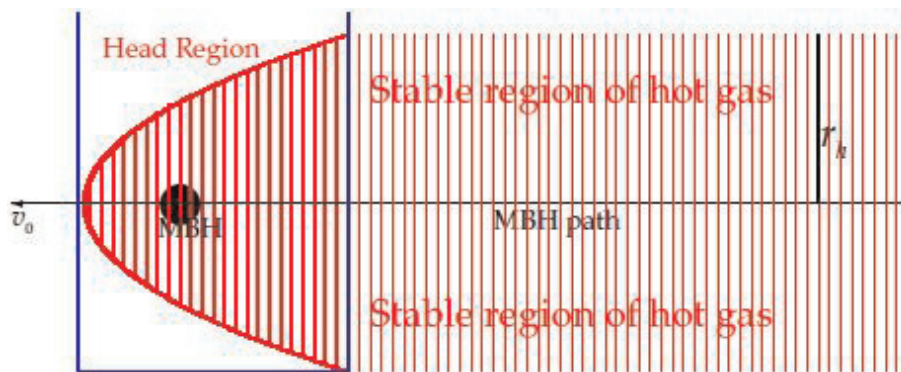


Figure 2.
 Heat wave caused by subsonic MBH.

In Eq. (A.3) above, acceleration due to MBH gravity at point \mathbf{r} is

$$\mathbf{g}(\mathbf{r}) = -MG \frac{\mathbf{r}}{\|\mathbf{r}\|^3} \quad (\text{A.4})$$

Substituting Eq. (A.4) into Eq. (A.3), we obtain

$$\mathbf{F} = -MG\rho \frac{K-1}{K} \iiint_{\mathcal{R}_{hg}} \frac{\mathbf{r}}{\|\mathbf{r}\|^3} dV, \quad (\text{A.5})$$

The gas displaced by the MBH passage in $-\hat{z}$ direction retains cylindrical symmetry. This symmetry implies that the net force on the MBH will act only in $-\hat{z}$ direction. Thus, Eq. (A.5) can be further simplified to

$$\begin{aligned} F_r &= -\mathbf{F} \cdot \hat{z} = MG\rho \frac{K-1}{K} \iiint_{\mathcal{R}_{hg}} \frac{\mathbf{r} \cdot \hat{z}}{\|\mathbf{r}\|^3} dV = MG\rho \frac{K-1}{K} \iiint_{\mathcal{R}_{hg}} \frac{z}{(z^2 + r^2)^{3/2}} dV \\ &\geq MG\rho \frac{K-1}{K} \int_0^{r_h} \int_{r_h}^{\infty} \frac{\pi r z}{(z^2 + r^2)^{3/2}} dz dr = \pi MG\rho \frac{K-1}{K} \int_0^{r_h} \left[-\frac{r}{\sqrt{z^2 + r^2}} \right]_{z=r_h}^{z=\infty} dr \\ &= \pi MG\rho \frac{K-1}{K} \int_0^{r_h} \frac{r}{\sqrt{r_{h_2}^2 + r^2}} dr = \pi MG\rho \frac{K-1}{K} \left[\sqrt{r_{h_2}^2 + r^2} \right]_{r=0}^{r_h} \\ &= \pi MG\rho r_h \left(\frac{K-1}{K} (\sqrt{2} - 1) \right). \end{aligned} \quad (\text{A.6})$$

As we have mentioned earlier, the real force is greater or equal to the one calculated by approximating \mathcal{R}_{hg} by Eq. (A.1). Eqs. (A.6) and (9), we obtain

$$r_1 \geq \frac{3}{2} (\sqrt{2} - 1) \frac{K-1}{K} r_h \approx 0.62 \frac{K-1}{K} r_h. \quad (\text{A.7})$$

Below, r_h is estimated in terms of r_2 . The power needed to heat the gas trail is

$$\begin{aligned} P_T &= (\text{Mass heated per unit of time}) \cdot (\text{Temperature}) \cdot C_p \\ &= v_0 \left(\pi r_{h_2} \frac{\rho}{K} \right) ((K-1)T) \left(\frac{5}{3} C_v \right) = \frac{5(K-1)}{3K} \pi v_0 \rho T C_v r_{h_2}, \end{aligned} \quad (\text{A.8})$$

where P_T is the thermal power. For monatomic gas, $C_p = \frac{5}{3} C_v$. Some of the power P radiated by the MBH goes into the production of the sonic waves, hence $P > P_T$. Accurate calculation of P_T/P is beyond the scope of this work. Nevertheless, for subsonic MBH, we are certain that no more than 20% of MBH heating power is consumed by making sonic waves. Therefore, $P_T/P \gtrsim 0.8$. Using this data, we estimate the total radiative power of MBH:

$$P \leq \frac{2(K-1)}{K} \pi v_0 \rho T C_v r_{h_2} \quad (\text{A.9})$$

Substituting Eq. (A.9) into Eq. (10), we obtain

$$\frac{2(K-1)}{K} \pi v_0 \rho T C_v r_{h_2} \geq \pi v_0 \rho T C_v r_{2_2}. \quad (\text{A.10})$$

Hence,

$$r_2 \leq r_h \sqrt{\frac{2(K-1)}{K}}. \quad (\text{A.11})$$

Dividing Eq. (A.7) by Eq. (A.11), we obtain

$$\eta_G = \frac{r_1}{r_2} \geq .44 \sqrt{\frac{K-1}{K}}. \quad (\text{A.12})$$

Calculation of K is beyond the scope of this work. Some considerations regarding the value of K are presented in Appendix A.2.

A.2 Estimation of K

Recall, that the average temperature of the gas in the hot tail is KT , where T is the temperature of the surrounding stellar material. In order to make any inference on the value of K , we introduce two radii and calculate their ratio. **Radiation radius** r_γ is the average distance traveled by a photon or another energy-carrying particle from PBH before being absorbed by stellar material. **Minimal hot tail radius** r_{mh} is the minimal radius the hot tail can have regardless of K .

Below we estimate r_γ and r_{mh} . The radiation radius is

$$r_\gamma = \frac{\mathfrak{S}_\gamma}{\rho_p} = \frac{\mathfrak{S}_\gamma}{10^3 \frac{\text{kg}}{\text{m}^3} \rho_{3p}}, \quad (\text{A.13})$$

where \mathfrak{S}_γ is the planar density of material through which an energy carrying particle has to travel before being absorbed by stellar material. The density ρ_p is an average density of the material over the path of the energy-carrying particle, and ρ_{3p} is the same density in 10^3kg/m^3 . The value of \mathfrak{S}_γ is inversely proportional to average absorption cross-section of the energy-carrying particles:

$$\mathfrak{S}_1 = \frac{1 \text{ kg}}{1000 N_A \text{ amu}} \cdot \frac{1}{10^{-28} \sigma} = \frac{17 \frac{\text{kg}}{\text{m}^2}}{\sigma \text{ in barn}}, \quad (\text{A.14})$$

where σ is the absorption cross-section. Given that most interactions are scattering, effective absorption cross-section has to be calculated. Substituting Eq. (A.14) into Eq. (A.13), we obtain

$$r_\gamma = \frac{\mathfrak{S}_\gamma}{\rho_p} = \frac{0.017 \text{ m}}{\rho_{3p}(\sigma \text{ in barn})}. \quad (\text{A.15})$$

According to data presented in ([17], pp. 41–42), cross-section per amu decreases with photon energy. For 10 keV photon, it is 0.55 barn For 1 MV photon, it is 0.18 barn. For 50 MV photon, it is 0.023 barn.

The minimal hot tail radius can be obtained from Eq. (A.8):

$$r_{mh} = \sqrt{\frac{3P_T}{5\pi v_{0\rho} TC_v}}, \quad (\text{A.16})$$

where P_T is the part of MBH power used to produce heat rather than the sound wave. Substituting Eqs. (15)–(17) into Eq. (12) we obtain

$$P_T = \eta_h P = \eta_h \eta_\Gamma \eta_A \frac{4\pi(MG)^2 c^2 \rho}{(v_{0_2} + v_{s_2})^{3/2}} = \eta_h \eta_\Gamma \eta_A \frac{4\pi(MG)^2 c^2 \rho}{v_{0_3} (1 + \mathcal{M}^{-2})^{3/2}}, \quad (\text{A.17})$$

where $\eta_h \approx 0.8$ is the fraction of MBH radiative power which goes into heating the stellar medium rather than producing a sonic wave. Substituting Eq. (A.17) into Eq. (A.16), we obtain

$$r_{mh} \approx 1.5 \sqrt{\eta_\Gamma \eta_A} \frac{MGc(1 + \mathcal{M}^{-2})^{-3/4}}{v_{0_2} \sqrt{TC_v}} \quad (\text{A.18})$$

As mentioned in Subsection 2.2, for average stellar material, $C_v = 2.01 \cdot 10^4 \frac{J}{kg^\circ K}$. From Eq. (A.18), we obtain

$$r_{mh} \approx (0.21 \text{ m}) \sqrt{\eta_\Gamma \eta_A} (1 + \mathcal{M}^{-2})^{-3/4} M_{18} v_{6_{-2}} T_{6_{-1/2}}. \quad (\text{A.19})$$

Combining Eq. (A.15) and Eq. (A.19), we obtain the ratio

$$\mathcal{R}_\gamma = \frac{r_\gamma}{r_{mh}} \approx 0.8 \frac{v_{6_2} \sqrt{T_6} (1 + \mathcal{M}^{-2})^{3/4}}{\rho_{3p} M_{18} (\sigma \text{ in barn}) \sqrt{\eta_\Gamma \eta_A}} \approx \frac{\sqrt{v_6 T_6} (\max\{v_6, v_{6s}\})^{3/2}}{\rho_{3p} M_{18} (\sigma \text{ in barn}) \sqrt{\eta_\Gamma \eta_A}}, \quad (\text{A.20})$$

where v_{6s} is the sound velocity in 10^6 m/s.

If $\mathcal{R}_\gamma \ll 1$, then gas close to MBH is heated to a great temperature. This gas expands before it has time to diffuse its heat. The expanded gas must remain hot in order to balance the outside pressure. In that case, $K \gg 1$. For $\mathcal{R}_\gamma \gg 1$, thermal energy is dissipated over a very large gas volume. This gas volume is heated only by a small margin, thus $0 < K - 1 \ll 1$.

B. Estimation of a MBH kinetic energy loss on passage through a sun-like star

Using $r_{\min} = 0.1 \text{ m}$ and $r_{\max} = 5 \cdot 10^7 \text{ m}$ to express Eq. (3) in numerical terms we obtain:

$$F_t = \frac{4\pi(MG)^2 \rho}{v_{0_2}} \ln \left(\frac{r_{\max}}{r_{\min}} \right) = (1.12 \cdot 10^9 \text{ N}) \frac{M_{18_2} \rho_3}{v_{6_2}}, \quad (\text{B.1})$$

where ρ_3 is density in 10^3 kg/m^3 , and v_6 is velocity in 10^6 m/s . Below, we tabulate several parameters for a MBH passing through a sun-like star. We use the density data from Solar interior given in [11]. Column 1 contains the fraction of Solar radius. Column 2 contains the gas density in 10^3 kg/m^3 . Column 3 contains an estimated

R_{Sun}	ρ_3	v_6	F_t/M_{18_2}
0.0	146	1.39	$85 \cdot 10^9 N$
0.1	82	1.33	$51 \cdot 10^9 N$
0.2	35	1.19	$28 \cdot 10^9 N$
0.3	12.3	1.06	$12.3 \cdot 10^9 N$
0.4	4.0	0.96	$4.9 \cdot 10^9 N$
0.5	1.35	0.87	$2.0 \cdot 10^9 N$
0.6	0.49	0.80	$0.86 \cdot 10^9 N$
0.7	0.185	0.74	$0.38 \cdot 10^9 N$
0.8	0.077	0.69	$0.18 \cdot 10^9 N$

Table 1.
 Parameters for MBH passing through a sun-like star.

speed of a MBH arriving from a distance of thousands of solar radii. Column 4 contains F_t for $M_{18} = 1$ (**Table 1**).

The Solar radius is $R_{\odot} = 6.96 \cdot 10^8 m$. Thus, we estimate the energy loss of a MBH passing through the center of a Sun-like star:

$$\Delta E = \int_{-R_{\odot}}^{R_{\odot}} F_t dx = (2.0 \cdot 10^{19} J)M_{18_2}. \quad (\text{B.2})$$


Author details

Mikhail V. Shubov

Department of Mathematics, University of Massachusetts Lowell, Massachusetts, USA

*Address all correspondence to: mvs5763@yahoo.com

IntechOpen

© 2022 The Author(s). Licensee IntechOpen. This chapter is distributed under the terms of the Creative Commons Attribution License (<http://creativecommons.org/licenses/by/3.0>), which permits unrestricted use, distribution, and reproduction in any medium, provided the original work is properly cited. 

References

- [1] Khriplovich IB, Pomeransky AA, Prodit N, Ruban GY. Can one detect passage of small black hole through the earth? *Physical Review D*. 2008;**77**(6):1-6
- [2] Pania P, Loebb A. Tidal capture of a primordial black hole by a neutron star: Implications for constraints on dark matter. *Journal of Cosmology and Astroparticle Physics*. 2014;**06**(2014):026
- [3] Carr B, Kuhnel F, Sandstad M. Primordial black holes as dark matter. *Physical Review D*. 2016;**94**:1-32
- [4] Bramante J. Dark matter ignition of type Ia supernovae. *Physical Review Letters*. 2015;**115**(14):1-6
- [5] McDermott SD, Yu HB, Zurek KM. Constraints on scalar asymmetric dark matter from black hole formation in neutron stars. *Physical Review D*. 2012;**85**(2):1-24
- [6] Abramowicz M, Becker J. No observational constraints from hypothetical collisions of hypothetical dark halo primordial black holes with galactic objects. *Astrophysical Journal*. 2009;**705**(1):659-669
- [7] Beckmann RS, Devriendt J, Slyz A. Bondi or not Bondi: The impact of resolution on accretion and drag force modelling for supermassive black holes. *Monthly Notices of the Royal Astronomical Society*. 2018;**478**(1):995-1016
- [8] Sánchez-Salcedo FJ, Brandenburg A. Dynamical friction of bodies orbiting in a gaseous sphere. *Monthly Notices of the Royal Astronomical Society*. 2001;**322**(1):67-78
- [9] Ostriker EC. Dynamical friction in a gaseous medium. *The Astrophysical Journal*. 1998;**513**(1):252-258
- [10] Bodenheimer PH. *Principles of Star Formation*. Berlin, Heidelberg: Springer Verlag; 2011
- [11] Guenther DB, Demarque P, Kim Y-C, Pinsonneault MH. Standard solar model. *The Astrophysical Journal*. 1992;**387**:372-393
- [12] Williams D. *Molecular Physics*. New York: Academic Press; 1961
- [13] Chakrabarti SK. *Accretion Processes on a Black Hole*. Bombay, India: Tata Institute of Fundamental Research; 1996
- [14] Chattopadhyay I, Sarkar S. General relativistic two-temperature accretion solutions for spherical flows around black holes. *International Journal of Modern Physics*. 2018;**28**(02):1950037
- [15] Colpi M, Maraschi L, Treves A. Two-temperature model of spherical accretion onto a black hole. *The Astrophysical Journal*. 1984;**280**:319-327
- [16] Kocsis B, Loeb A. Menus for feeding black holes. *Space Science Reviews*. 2014;**183**(1-4):163-187
- [17] Hubbell JH. *Photon Cross Sections, Attenuation Coefficients, and Energy Absorption Coefficients from 10 Key to 100 GeV*. Washington D.C.: Center for Radiation Research National Bureau of Standards; 1969
- [18] Tinyakov P, Kouvaris C. Growth of black holes in the interior of rotating neutron stars. *Physical Review D*. 2013;**90**(4):043512
- [19] Contopoulos I, Gabuzda D, Kylafis N. *The Formation and Disruption of Black Hole Jets*. Berlin/Heidelberg: Springer; 2015. pp. 1-9

[20] Zhang B. *The Physics of Gamma-Ray Bursts*. Cambridge: Cambridge University Press; 2018

[21] Lide DR. *CRC Handbook of Chemistry and Physics*. 84th ed. Boca Raton, Florida: CRC Press; 2003

[22] Ambastha A. Probing the solar interior: Hearing the heartbeats of the sun. *Resonance*. 1998;3(3):18-31

IntechOpen